Constraining Particle Physics Models with Supernovae Observations

A thesis submitted in partial fulfillment of the requirement
for the degree of Bachelor of Science with Honors in
Physics from the College of William and Mary in Virginia,

by

Keith C. Bechtol

Accepted for _____

_____
Advisor: Joshua Erlich

_____
Gina Hoatson

_____
Christopher Carone

_____
Nicholas Loehr

Williamsburg, Virginia
April 30, 2007

Abstract

Three particle physics theories are evaluated based upon their consequences for cosmology. Observations of type Ia supernovae supplied by the Supernova Legacy Survey and Hubble Space Telescope are used to constrain the parameters of the proposed models. First, a cosmological model incorporating photon-axion oscillations is tested. When combined with cosmic microwave background and baryon acoustic oscillation constraints, supernovae data restricts the decay length of photons to be greater than 7000 Mpc. Next, we consider the possibility of dust on a negative tension brane in a Randall-Sundrum braneworld scenario. The effective equation of state relating pressure, p, to density, ρ, for the matter on the negative tension brane would be $p = \frac{1}{5}\rho$. Letting w denote the equation of state parameter, we have $w_{(-)} = \frac{1}{5}$. Substances with positive equation of state parameters are ruled out by Big Bang nucleosynthesis. However, we find that supernovae data alone is inconsistent with the the existence of substances with $w = \frac{1}{5}$. Finally, we test the possibility of topological defects from GUT symmetry breaking. Relics of this symmetry breaking include cosmic strings and domain walls with equation of state parameters $w_{CS} = -\frac{1}{3}$ and $w_{DW} = -\frac{2}{3}$ respectively. For both types of topological defects, the allowed energy density is comparable to the matter density of the Universe.

Acknowledgements

The author would like to thank Professor Joshua Erlich of the College of William and Mary for describing and discussing numerous cosmology and particle physics models. This project would not have been possible nor nearly as enjoyable without his guidance.

Contents

1 Introduction

Many contemporary particle physics theories have far-reaching and surprising consequences for other areas of physics. For example, observations of the galaxy clusters suggest that an additional long-range force between dark matter particles may be needed to explain rapid galactic accelerations [1]. One might wonder what role new particles and interactions could play in the behavoir of the Universe as a whole. In this paper, we examine three particle physics theories in the context of their implications for cosmology. The predictions of each theory will be compared to recent type Ia supernovae observations from the Supernova Legacy Survey and the Hubble Space Telescope. Type Ia supernovae are important astronomical events because their intrinsic luminosity is predictable throughout the observable Universe. Therefore, the redshift and the apparent brightness of type Ia supernovae can provide independent measures of cosmological distances. The combination of these two distance measurements is used to study the expansion history of the Universe. Statistical analyses of cosmological models including photon-axion oscillations, Randall-Sundrum braneworlds, and topological defects from symmetry breaking will be conducted in the following study. The reevaluation of supernovae observations in light of the new particle physics theories will also be used to constrain cosmological parameters in each of these cases. The fits of cosmological parameters can then be compared to observations of the cosmic microwave background radiation from the most recent Wilkinson Microwave Anisotropy Probe (WMAP) three-year study and measurements of large scale structure from the Sloan Digital Sky Survey (SSDS).

2 Type Ia Supernovae

Type Ia supernovae occur in binary star systems in which a white drawf star accretes mass from its partner star, typically a red giant. When the mass of the white dwarf

star surpasses the Chandrasekhar mass limit of about 1.4 solar masses, a stellar explosion occurs. Due to this consistent process, the intrinisic luminosities of these events are nearly uniform throughout the observable universe because of the fixed mass of the exploding star. The distance of type Ia supernovae can be measured using two independent methods. First, the consistent intrinsic luminosities of these explosions allows type Ia supernovae to be used as standard candles. The dimmer the object appears from Earth, the greater the observing distance. For a given cosmological model, the measured bightness of supernovae can be used to determine cosmological distances. Secondly, the redshift of the spectra of type Ia supernovae provides information about the expansion of space between the supernovae and the Earth since the time of the explosion. Therefore, the relationship between the observed supernovae luminosity and redshift can be used to trace back the expansion history of the Universe and to constrain the parameters of cosmological models.

As alluded to previously, the intrinsic luminosities of type Ia supernovae are not completely uniform. However, the light curves of type Ia supernovae (appearent luminosity as a function of time) can be used to increase the accuracy of intrinsic luminosity estimates. Supernovae brightness rises gradually and then diminishes over the period of roughly a month. To a first approximation, only the peak luminosity is considered when determining intrinsic luminosity. The phenomenologically based Phillips Curve uses a stretch factor to relate the time-width of light curves to the intrinsic luminosity of the supernovae [2]. In short, supernovae events of longer duration tend to be brighter as well. This model was empirically generated from studies of nearby supernovae in which the observing distance could be accurately determined by other methods such as parallax. In addition, supernovae with a bluer light sprectrum are also intrinsically brighter. Both the brighter-slower and brighter-bluer correlataions must be taken into account in order to accurately gauge the intrinsic luminosities of type Ia supernovae.

2.1 Supernova Legacy Survey

The supernovae observations considered in this analysis are supplied by the Supernova Legacy Survey and the Hubble Space Telescope. The Supernova Legacy Survey includes data from 44 nearby ($z \leq 0.125$, see redshift definition equation (3.2)) and 73 high-redshift ($z \geq 0.2$) type Ia supernovae [2]. The observational program consisted of two parts. First, the MegaCam instrument of the Canada-France-Hawaii Telescope identified supernovae and recorded light curves. Next, the Very Large Telescope and the Gemini and Keck telescopes performed a spectroscopic follow-up of supernovae to confirm the events and to take redshift measurements. The Supernova Legacy Survey data set lists both the original observed magnitudes of supernovae and the corrected magnitudes to adjust for brighter-slower and brighter-bluer effects to intrinsic luminosity. The parameters used in models accounting for bright-slower and brighter-bluer correlations were fitted to light curves of nearby supernovae [2].

2.2 Hubble Space Telescope

An additional 21 type Ia supernovae discovered by the Hubble Space Telescope compliment the data sample of the Supernova Legacy Survey [3]. The observations include 13 supernovae with redshift $z \geq 1$. When combining data sets, the spectrophotometric systems used in each study must be considered in order to compare observed magnitudes. Both the Supernova Legacy Survey and the Hubble Space Telescope experiment utilized the the Vegamag photometric system and Landolt calibration system to record their findings [2, 3]. The Vegamag photometric system selects Vega as a reference point for all stellar magnitudes. The Landolt calibration system allows for calibration between B, V, R, and I filter band passes. The adoption of common spectrophotometric methods allows for the two sets of supernovae observations to be analyzed together. With a sample of 138 type Ia supernovae observations at hand, we now outline the basic cosmological model used to describe the overall behavoir of

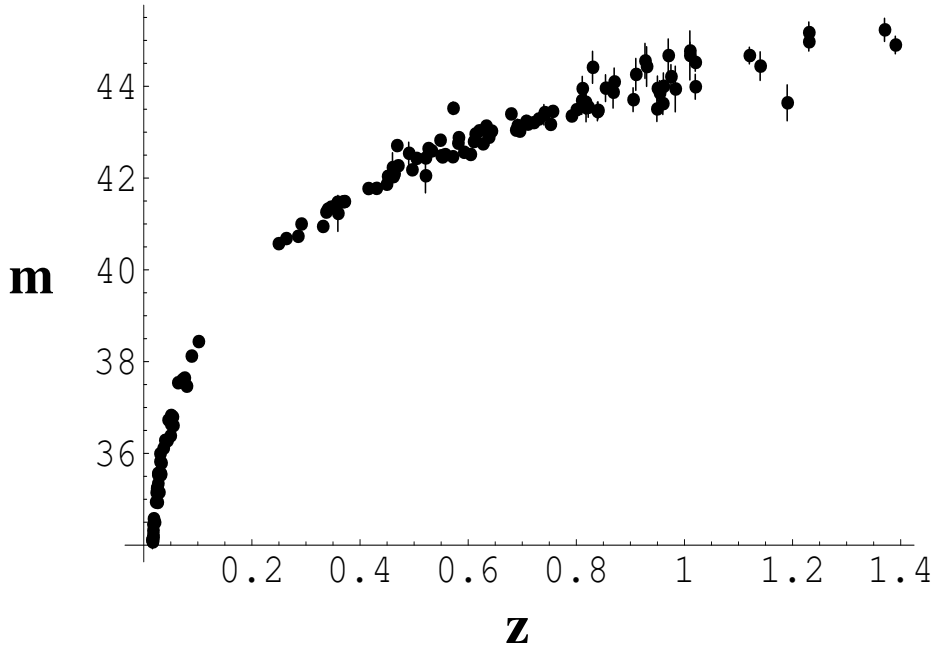

Figure 1: The observed magnitude, m, and redshift, z, of 135 type Ia supernovae are shown in the Hubble diagram above. Error bars are included. The plot contains supernovae data points from both the Supernova Legacy Survey and Hubble Space Telescope experiments.

the Universe.

A Hubble diagram showing observed magnitude, m, versus redshift, z, for the combined Supernova Legacy Survey and Hubble Space Telescope data sets is contained in Figure 1. The observed magnitude is related to brightness on a logarithmic scale in which brighter objects have lower magnitudes (see equation (5.2) for a definition of magnitude).

3 Cosmological Models

The Universe exhibits vast differences in ranges of energy density on relatively small scales. For example, consider the energy density difference between the cores of stars compared to the nearly empty regions of space between galactic clusters. However,

the combination of the Copernican Assumption (stating that there are no preferred spatial locations) and observed isotropy (the Universe appears the same in all directions) suggests that the Universe must be homogeneous on the largest scales. The homogeneous condition motivates the use of a maximally symmetric metric to describe the space-time geometry of the entire universe. The Robertson-Walker metric,

$$ds^2 = -c^2dt^2 + R_o^2a^2(t)\left(\frac{dr^2}{1-kr^2} + r^2d\theta^2 + r^2\sin^2\theta d\phi^2\right), \tag{1}$$

incorporates this spatial symmetry and allows for the time evolution of the Universe. The metric provides information on cosmological distances where t represents the time dimension and r, θ, and ϕ indicate spatial dimensions. The quantity R_o characterizes the absolute size of the Universe and the scale factor $a(t)$ encodes the expansion history of the universe. We define the scale factor at the present time $t = 0$ to be $a(0) \equiv a_o = 1$. The variable k represents the curvature of the Universe and can attain the values -1, 0, or 1 depending on whether the Universe is open, flat, or closed, respectively.

The redshift is related to the scale factor by

$$z = \frac{1}{a} - 1 \text{ or } a = \frac{1}{1+z}, \tag{2}$$

where the convention $a_o = 1$ implies that the redshift of photons emitted today is $z_o = 0$. Next, we want to relate the geometry of the Universe to its contents. This is accomplished by solving Eistein equations:

$$R_{\mu\nu} = 8\pi G(T_{\mu\nu} - \frac{1}{2}g_{\mu\nu}T). \tag{3}$$

On the left side of equation (3.3), the Ricci tensor $R_{\mu\nu}$ depends only on the geometry of the Universe as defined by the Robertson-Walker metric. Note that Greek indicies will run from 0 to 3 and that Latin indices will run from 1 to 3. The energies, momenta, and pressures of substances in the Universe are encoded on the right side

of Einstein's equations. Newton's gravitational constant is symbolized by G. We assume that the matter and energies of cosmological interest behave as perfect fluids. As a result of isotropy, the perfect fluids appear to be at rest in comoving coordinates and the four-velocity can be written as $U^\mu = (1, 0, 0, 0)$, setting the speed of light $c = 1$. The energy-momentum tensor $T_{\mu\nu} = (\rho + p)U_\mu U_\nu + p g_{\mu\nu}$ will become

$$T_{\mu\nu} = \begin{pmatrix} \rho & 0 & 0 & 0 \\ 0 & & & \\ 0 & & g_{ij}p & \\ 0 & & & \end{pmatrix} \tag{4}$$

where ρ and p indicate the pressure and density of the substances respectively and $g_{\mu\nu}$ is the metric tensor. The equation of state parameter w relates the pressure and energy density of a particular substance. Perfect fluids are described by $p_i = w_i \rho_i$. In addition, we have a statement for the conservation of energy,

$$\dot{\rho_i} + 3(\rho_i + p_i)H = 0 \text{ or equivalently } \frac{\dot{\rho}}{\rho} = -3(1 + w)\frac{\dot{a}}{a}, \tag{5}$$

because the energy-momentum tensor must be covariantly conserved. Solutions to equation (3.5) have the form

$$\rho_i = \rho_{i,o}(1 + z)^{3(1+w_i)}. \tag{6}$$

For our basic cosmological model, we will consider three types of substances in the Universe. First, matter acts as a pressureless dust with an equation of state parameter $w_M = 0$. Note that the vast majority of matter in the Universe exists in the form of nonbaryonic dark matter. Next, radiation type substances such as photons and relativistic massive particles (example: neutrinos) are described by a traceless energy-momentum tensor in accordance with electromagnetism. The trace of the energy-momentum tensor is $T = -\rho + 3p$. Thus, the equation of state parameter

for radiation is $w_R = \frac{1}{3}$. Finally, the term dark energy refers to any substance with a negative-valued equation of state parameter. Let w_Λ denote the equation of state parameter for dark energy.

The solutions to the Einstein equations using the Robertson-Walker metric and the energy-momentum tensor given by equation (3.4) yield the Friedmann equation

$$H^2 = \left(\frac{\dot{a}}{a}\right)^2 = \frac{8\pi G}{3c^2}\sum_i \rho_i - \frac{kc^2}{a^2 R_o^2}, \tag{7}$$

with the Hubble paramter defined as $H \equiv \frac{\dot{a}}{a}$. Next, we introduce the density parameter, Ω, defined as

$$\Omega_i = \frac{8\pi G}{3H^2}\rho_i. \tag{8}$$

In terms of the density parameters, the Friedmann equation can be written in a new form in which the relationship between the sum of the density paramters and the curvature is more evident:

$$\sum_i \Omega_i - 1 = \frac{kc^2}{H^2 a^2}. \tag{9}$$

Define the critical density such that the spatial curvature is equal to zero when the density parameters are summed together. This situation corresponds to a flat Universe. We write,

$$\Omega_i = \frac{\rho_i}{\rho_{crit}} \text{ with } \rho_{crit} \equiv \frac{3c^2 H^2}{8\pi G}. \tag{10}$$

The Friedmann equation gives the Hubble parameter in terms of the scale factor. However, we would like to express this quantity as a function of the redshift for future calculations. The quantity H_o indicates the Hubble Constant as determined at the present time. The measured value for the Hubble Constant is 72 ± 5 kilometers per second per megaparsec [4]. Substituting the redshift for the scale factor, the Hubble parameter can now be expressed as

$$H^2(z) = H_o^2(1+z)^2\left[1+\sum_i \Omega_i\left((1+z)^{1+3w_i}-1\right)\right]. \tag{11}$$

Now consider the path of photons emitted from a distant source travelling towards the Earth. We know that photons move along null geodesics with $ds^2 = 0$. If the photons propogate radially outward from the source, then we have $d\theta^2 = 0$ and $d\phi^2 = 0$ as well. In that case, the proper time of a light ray vanishes and the Friedmann-Robertson-Walker cosmology becomes

$$0 = -c^2dt^2 + R_o^2a^2(t)\frac{dr^2}{1-kr^2}. \tag{12}$$

Rearranging equation (3.12) and noting that $H(z) = \frac{\dot{a}}{a} = \frac{\dot{z}}{z+1} = a\dot{z} = a\frac{dz}{dt}$, we find that

$$\frac{dr}{\sqrt{1-kr^2}} = \frac{cdt}{R_oa(t)} = \frac{cdz}{R_oH(z)}. \tag{13}$$

Integrating equation (3.13) we obtain

$$\int_0^{r_s}\frac{dr}{\sqrt{1-kr^2}} = \int_{t_s}^{0}\frac{cdt}{R_oa(t)} = \int_0^{z_s}\frac{cdz}{R_oH(z)}. \tag{14}$$

The most recent WMAP three-year study has confirmed that the Universe appears to be spatially flat, implying that the curvature is equal to zero [4]. After substituting for $H(z)$, the integral of equation (3.14) yields an equation for the comoving distance $r_s(z_s)$:

$$r_s(z_s) = \frac{c}{R_oH_o}\int_0^{z_s}\frac{dz}{(1+z)\sqrt{1+\sum_i \Omega_i\left((1+z)^{1+3w_i}-1\right)}}. \tag{15}$$

The equation for the comoving distance gives the propogation distance of photons traveling over extragalactic distances in terms of the redshift. The absolute distance is recovered by multiplying the comoving distance by R_o. We now have a relationship

between distance and redshift that depends on the cosmological density parameters and the equation of state parameters of the contents of the Universe.

Several experimental efforts have already adressed the question of the composition of the Universe. Using the Cosmological Concordance Model, the WMAP three-year study found that the matter density $\Omega_M = 0.27 \pm 0.04$ and that the equation of state for dark energy $w_\Lambda = -0.98 \pm 0.12$ [4]. These parameter values will provide a reference as we proceed with the analysis of particle physics theories.

4 Particle Physics Theories

Three particle physics theories will be evaluated based on how well their cosmological implicatations match with type Ia supernovae observations. We will discuss, in order, the theoretical background and cosmological effects of photon-axion oscillations, the existence of shadow matter in a Randall-Sundrum braneworld scenario, and cosmic scale topological defects from symmetry breaking.

4.1 Photon-Axion Oscillations

Supernovae observations in conjunction with contemporary cosmological models suggest that the Universe is dominated by dark energy and that the expansion rate of the Universe is accelerating exponentially [5]. However, the cosmological constant problem motivates the search for alternative explainations for the apparent accelerated expansion. The current understanding of field theory predicts a value for the cosmological constant that is 120 orders of magnitude too large to be reconciled with cosmology observations. Perhaps, scalar fields do not couple to gravity as expected and do not contribute to the cosmological constant. This scenario would alleviate the cosmological constant problem but requires a new interpretation of supernovae data. One approach is to consider the possibility of a dimming mechanism such that

distant supernovae are not as bright as anticipated by traditional cosmological models. Several observations place limitations on these types of theoretical proposals. First, the absence of significant frequency gaps or other chromatic discrepancies in supernovae spectra requires uniform dimming across the optical range of the electromagnetic spectrum. This effect reduces the likelihood that light is scattered by matter particles. Also, reemitted infrared light from interactions between photons and intergalactic dust would be highly conspicuous in the cosmic microwave background radiation [6].

A more promising dimming mechanism is a type of flavor oscillation involving photons. To this end, Csaki, Kaloper, and Terning have proposed a model in which photons can oscillate into axions in the presence of external magnetic fields [5, 6, 7]. According to their model, the electromagnetic field can couple with the scalar axion field. The Lagrangian of the photon-axion interaction is given by

$$L_{int} = \frac{\phi}{M_L c^2} \vec{E} \cdot \vec{B}, \tag{16}$$

where M_L signifies the coupling strength of the interaction and $\vec{E}$ and $\vec{B}$ represent the electric and magnetic fields. Solutions to the resulting Langrange equations have oscillatory forms in the presence of a background magnetic field. The strength of the interactions depends on the axion mass. Historically, the axion particle was proposed to answer the strong CP problem with a mass in the range of $10^{-5} \frac{\mathrm{eV}}{c^2}$ to $10^{-1} \frac{\mathrm{eV}}{c^2}$. However, the mass scale of axions in the model suggested by Csaki, Kaloper, and Terning is closer to $10^{-16} \frac{\mathrm{eV}}{c^2}$ [6]. This smaller axion mass scale is chosen in order to leave the cosmic microwave background unaffected. Notice that the existence of an external magnetic field is required in equation (4.1) to allow for a nonzero scalar product in the Langrangian such that mixing between photon and axion eigenstates can occur. However, weak magnetic fields do indeed permeate the vast regions of space between galaxies [8]. These extragalactic magnetic fields are randomly oriented

with domain sizes on the order of megaparsecs. Also, the field strength appears to be relatively uniform throughout the magnetic domains. Csaki, Kaloper, and Terning employ the approximation that photons traversing great distances will encounter numerous magnetic domains such that the random orientations balance each other for a net dimming effect of distant light sources [7].

In the high energy limit relevant to optical photons, both the oscillation amplitude and oscillation length become less dependent on the specific photon energy. As a result, the flavor mixing distributes the originally unpolarized photons evenly across three mass eigenstates: two photon polarization states, and one axion state. Thus, the fraction of emitted photons that remain as photons asymptotes towards $\frac{2}{3}$ over large distances [7]. After a series of calculations, Csaki, Kaloper, and Terning determine that the survival probability of high energy photons as a function of propogation distance can be written as

$$P_{\gamma\to\gamma}(l) \cong \frac{2}{3} + \frac{1}{3}e^{-l/L_{decay}}, \tag{17}$$

where l represents the distance traveled by photons and L_{decay} denotes the decay length of photons [6]. In the high energy limit, the decay length is approximated by

$$L_{decay} = \frac{8}{3}\frac{\hbar^2 c^6 M_L^2}{L_{dom}|\vec{B}|^2}. \tag{18}$$

The average intergalactic magnetic field domain size is measured to be $L_{dom} \sim 1\text{Mpc}$ and the intergalactic magnetic field strength is roughly 10^{-13} tesla such that the magnetic field strength given in units of energy squared is $|\vec{B}|^2 \sim 10^{-13}\text{T}\sqrt{4\pi\varepsilon_o\hbar^3c^5}$ [8]. As a convention in this paper, we will express the decay length as a multiple of the theoretical decay length suggested by Csaki, Kaloper, and Terning: $L_{th} \cong 3600\text{Mpc}$ [6].

4.2 Randall-Sundrum Braneworlds

The Randall-Sundrum braneworld scenario proposes a new geometry to describe the Universe. The theory is a member of the larger class of Kaluza-Klein theories that posit the existence of extra spatial dimensions. According to Randall and Sundrum, Standard Model physics with the exception of gravity is confined to 4-dimensional spaces called branes embedded in a higher dimensional geometry [9]. In contrast, gravity can exist everywhere in the Randall-Sundrum braneworld. The Randall-Sundrum braneworld concept is motivated by an effort to explain the hierarchy problem in particle physics: an issue related to the scale of new gravitational physics and the puzzle of why gravity appears so weak in comparison to the other fundamental forces. In the theory, there exists a more fundamental scale of new gravitational physics that is multiplied by a factor related to brane tension and the distance between branes.

Despite our confinement on a particular brane, matter on other branes may still interact gravitationally with matter on our brane and produce observable effects [10]. Garriga and Tanaka call this matter existing on other branes shadow matter. Garriga and Tanaka study a particular braneworld scenario with one additional spatial dimension, y, and two branes. Their model proposes that we live on a positive tension brane located at $y = 0$ and that a negative tension brane exists at $y = d$. The five-dimensional Anti-deSitter space geometry of the braneworld is given by

$$ds^2 = g_{ab}dx^a dx^b = dy^2 + a^2(y)\eta_{\mu\nu}dx^\mu dx^\nu \tag{19}$$

with $a(y) = e^{-|y|/l}$. The four-dimensional Minkowski metric is symbolized by $\eta_{\mu\nu}$ and l indicates the curvature radius of Anti-deSitter space as related to brane tension. In this geometry, the apparent four-dimensional mass scale corresponding to new gravitational physics, $M_{4\mathrm{D}}$, is related to the fundamental mass scale, M_{F}, by

$$M_{4\mathrm{D}} \propto M_{\mathrm{F}} e^{\frac{d}{l}}. \tag{20}$$

Notice that as the factor $e^{\frac{d}{l}}$ becomes large, the apparent four-dimensional Planck scale grows rapidly. The relative adjustment of mass scales could help explain the hierarchy problem. The perturbed metric in this space is given by $\tilde{g}_{ab} = g_{ab} + h_{ab}$. This perturbation can be used to determine the effect of matter and energy on the metric and hence the effect of gravitational forces in a given metric space. In the Newtonian limit, we identify $h_{00} = -2\Phi$ so that we recover Poisson's equation for the gravitational field: $\nabla^2 h_{00} = -8\pi G\rho$ or $\nabla^2\Phi = 4\pi G\rho$. The gravitational interaction is generally characterized by the zero-mode (ground state) solution to the equations of motion with higher order modes representing corrections to the gravitational potential [9]. By solving the equations of motion in the braneworld geometry, Garriga and Tanaka [10] derive that the zero mode approximation to the gravitational field on each brane will satisfy

$$\left(\frac{1}{a^2}\Box^{(4)}\overline{h}_{\mu\nu}\right)^{(\pm)} = -\sum_{\sigma=\pm} 16\pi G^{(\sigma)}\left(T_{\mu\nu} - \frac{1}{3}\gamma_{\mu\nu}T\right)^{(\pm)} \pm \frac{16\pi G^{(\pm)}}{3}\frac{\sinh(d/l)}{e^{\pm d/l}}\gamma_{\mu\nu}T^{(\pm)}. \tag{21}$$

Garriga and Tanaka introduce $G^{(\pm)}$, a quantity related to Newton's constant in the new geometry by

$$G^{(\pm)} = \frac{G_5 l^{-1} e^{\pm d/l}}{2\sinh(d/l)}, \tag{22}$$

where G_5 denotes the five-dimensional Newton's constant. Also appearing in equation (4.6) is the background spatial metric, $\gamma_{\mu\nu}$, which is defined as

$$\gamma_{\mu\nu} = e^{-\frac{2|y|}{l}}\eta_{\mu\nu}. \tag{23}$$

The index σ in equations (4.6) and (4.7) selects the positive (plus sign) and negative (minus sign) tension branes. Using the theoretical framework developed by Randall, Sundrum, Garriga, and Tanaka, we can now calculate the gravitational influence of

matter on the negative tension brane. First, expand equation (4.6) for $d/l \gg 1$, the case in which the distance between branes is significantly larger than the brane tension. After performing this expansion, we find that the metric perturbation on the positive tension brane is a solution of

$$\frac{1}{a^2}\Box^{(4)}\overline{h}^{(+)}_{\mu\nu} = -16\pi G_5 l^{-1}\left[\left(T_{\mu\nu}-\frac{1}{2}\eta_{\mu\nu}T\right)^{(+)}+\left(T_{\mu\nu}-\frac{1}{3}\eta_{\mu\nu}T\right)^{(-)}e^{-\frac{2d}{l}}\right]. \quad (24)$$

The quantities in the parentheses marked by the plus and minus signs represent the contributions of matter and energy on the positive and negative tension branes respectively. For the contribution from the negative tension brane, we seek to identify an effective energy-momentum tensor structure, $T^{eff}_{\mu\nu}$, such that

$$T^{(-)}_{\mu\nu}-\frac{1}{3}\eta_{\mu\nu}T^{(-)} = T^{eff}_{\mu\nu}-\frac{1}{2}\eta_{\mu\nu}T^{eff}. \quad (25)$$

Here, the factor $e^{-\frac{2d}{l}}$ has been absorbed into $T^{eff}_{\mu\nu}$. Solving for the tensor structure of $T^{eff}_{\mu\nu}$, we find

$$T^{eff}_{\mu\nu} = \begin{pmatrix} \frac{5}{6}\rho & 0 & 0 & 0 \\ 0 & \frac{1}{6}\rho & 0 & 0 \\ 0 & 0 & \frac{1}{6}\rho & 0 \\ 0 & 0 & 0 & \frac{1}{6}\rho \end{pmatrix} = \frac{5}{6}\begin{pmatrix} \rho & 0 & 0 & 0 \\ 0 & \frac{1}{5}\rho & 0 & 0 \\ 0 & 0 & \frac{1}{5}\rho & 0 \\ 0 & 0 & 0 & \frac{1}{5}\rho \end{pmatrix} = \frac{5}{6}\begin{pmatrix} \rho & 0 & 0 & 0 \\ 0 & p & 0 & 0 \\ 0 & 0 & p & 0 \\ 0 & 0 & 0 & p \end{pmatrix}. \quad (26)$$

Using the equation of state, $p = w_{(-)}\rho$, we can identify $w_{(-)} = \frac{1}{5}$ from equation (4.11). Significant densities of substances with $w > 0$ are ruled out by cosmological observations in conjuction with Big Bang nucleosynthesis. However, we will constrain the amount of shadow matter existing on a negative tension brane using type Ia supernovae observations alone.

4.3 Topological Defects

The unification of the strong, weak, and electromagnetic forces is one of the great achievements of gauge theory. While this effect is most evident in particle accelerators today, in the early history of the Universe it is believed that the fundamental forces coupled together as a single interaction. As the Universe cooled, spontaneous symmetry breaking may have occured as early fields froze in particular orientations [11]. The Higgs field is one example of a field that may have acquired nonzero expectation value during this period. As the temperature decreased, the scalar field potential transitioned from having a single minumum value to having multiple possible minima. Thus, it became possible for two neighborhing regions of space to have differing field values corresponding to distinct ground states. The pattern of symmetry breaking may have produced topological defects whose gravitational effects would have cosmological consequences.

Cosmic strings and domain walls are two examples of cosmic vacuum structures associated with symmetry breaking [11, 12]. Domain walls are the two-dimensional structures that mark the boundaries between field domains. Cosmic strings are one-dimensional topological defects created during a different phase transition of symmetry breaking. In order to determine the macroscopic gravitational effects of topological defects, we calculate the energy-momentum tensor following the method of Vilenkin [12]. First, model a domain wall as an infinitely thin static plane located at $x = a$. The energy momentum-tensor of this configuration is

$$T_\mu^\nu(x) = \delta(x-a)\int \tilde{T}_\mu^\nu(x)dx, \tag{27}$$

where

$$\tilde{T}_\mu^\nu(x) = \sum_i \frac{\partial L}{\partial(\partial_\nu \phi^{(i)})}\partial_\mu \phi^{(i)} - \delta_\mu^\nu L \tag{28}$$

for fields $\phi^{(i)}$ and field Langragians $L(\phi^{(i)}, \partial_\mu \phi^{(i)})$. Note that in this geometry, the fields $\phi^{(i)}$ are functions only of x. An examination of equation (4.13) reveals that $T^\nu_\mu(x)$ can only have non-zero elements along the diagonal. Also, conservation of 4-momentum implies that

$$\partial_\beta T^\beta_\alpha = 0, \tag{29}$$

and in particular,

$$\frac{d}{dx} T^1_1(x) = 0. \tag{30}$$

In other words, $T^1_1(x)$ is constant. However, equation (4.12) implies that $T^1_1(x) = 0$ for $x \neq a$. Hence, $T^1_1(x) = 0$. For the other diagonal terms, $T^\nu_\mu(x)$ can only be non-zero at $x = a$ and since the fields $\phi^{(i)}$ are functions only of x, we observe that

$$T^0_0(x) = T^2_2(x) = T^3_3(x). \tag{31}$$

If we let σ denote the surface energy density, then the domain wall energy-momentum tensor can be written

$$T^\nu_\mu(x) = \delta(x-a) \begin{pmatrix} \sigma & 0 & 0 & 0 \\ 0 & 0 & 0 & 0 \\ 0 & 0 & -\sigma & 0 \\ 0 & 0 & 0 & -\sigma \end{pmatrix}. \tag{32}$$

Using equation (4.17), the energy-momentum tensor of a collection of domain walls with arbitrary orientations is

$$T^{\nu}_{\mu}(x) \propto \begin{pmatrix} \rho & 0 & 0 & 0 \\ 0 & -\frac{2}{3}\rho & 0 & 0 \\ 0 & 0 & -\frac{2}{3}\rho & 0 \\ 0 & 0 & 0 & -\frac{2}{3}\rho \end{pmatrix}. \tag{33}$$

Thus, we find that the equation of state for domain walls is $w_{DW} = -\frac{2}{3}$. The method of determining the energy-momentum tensor for cosmic strings follows a similar procedure. A single cosmic string will be modeled as an infinitely thin line located at $x = a$, $y = b$. The energy-momentum tensor for the string is

$$T^{\nu}_{\mu}(x, y) = \delta(x - a)\delta(y - b) \int \tilde{T}^{\nu}_{\mu}(x, y)dxdy, \tag{34}$$

where $\tilde{T}^{\nu}_{\mu}(x, y)$ is defined as before and now the fields $\phi^{(i)}$ are functions of both x and y. As in the domain wall case, $T^{\nu}_{\mu}(x, y)$ for a cosmic string can only have non-zero elements along the diagonals. Applying 4-momentum conservation, we observe that

$$\frac{d}{dx}T^1_1(x, y) = 0 \text{ and } \frac{d}{dy}T^2_2(x, y) = 0. \tag{35}$$

Therefore, both $T^1_1(x, y)$ and $T^2_2(x, y)$ are constant and since $T^{\nu}_{\mu}(x, y) = 0$ for $x \neq a$ or $y \neq b$ it is evident that

$$T^1_1(x, y) = T^2_2(x, y) = 0. \tag{36}$$

Also, equation (4.19) implies that

$$T^0_0(x, y) = T^3_3(x, y) \tag{37}$$

since $T^{\nu}_{\mu}(x, y)$ can only be non-zero at $x = a$ and $x = b$ and the fields are functions only of x and y. If we let λ denote the linear energy density of the cosmic string then the energy-momentum tensor of the cosmic string becomes

$$T^{\nu}_{\mu}(x,y) = \delta(x-a)\delta(y-b)\begin{pmatrix} \lambda & 0 & 0 & 0 \\ 0 & 0 & 0 & 0 \\ 0 & 0 & 0 & 0 \\ 0 & 0 & 0 & -\lambda \end{pmatrix}. \tag{38}$$

For a network of cosmic strings with arbitary orientations, the energy-momentum tensor of the network can be written as

$$T^{\nu}_{\mu}(x,y) \propto \begin{pmatrix} \rho & 0 & 0 & 0 \\ 0 & -\frac{1}{3}\rho & 0 & 0 \\ 0 & 0 & -\frac{1}{3}\rho & 0 \\ 0 & 0 & 0 & -\frac{1}{3}\rho \end{pmatrix}, \tag{39}$$

and one can read off the equation of state for a network of cosmic strings as $w_{CS} = -\frac{1}{3}$. In summary, when approximating the domain walls and cosmic strings as infinitely thin surfaces and curves, the equation of state parameters for collections of domain walls and cosmic strings are $w_{DW} = -\frac{2}{3}$ and $w_{CS} = -\frac{1}{3}$ respectively [12]. These two types of topological defects will be considered in fits to supernovae data to evaluate the proportion of vacuum energy of the Universe that could be composed of remnants of symmetry breaking.

5 Statistical Analysis

A statistical analysis is performed for each of the three theories. The basic procedure of the analysis is described in the methodology subsection and the unique aspects and results of each theory are covered in three separate results subsections. A total of 135 supernovae observations from the Supernova Legacy Survey and Hubble Space Telescope are used in each statistical analysis.

5.1 Methodology

Cosmological models are evaluated using goodness-of-fit tests to asses the level of agreement between supernovae observations and hypothesized predictions from models. Cosmological parameters will be estimated using the method of least squares and minimizing χ^2. For all of the models in this analysis, a flat Universe is assumed such that $\sum_i \Omega_i = 1$. Also, we assume that the radiation energy density is equal to zero, that is, $\Omega_R = 0$. The significance of cosmological models can be determined by examination of the minimized χ^2 values. The number of degrees of freedom, n_d, is equal to the number of measurements, N, minus the number of fitter parameters. Reasonable hypothesis should produce χ^2_{min} values in the neighborhood of the number of degrees of freedom.

In general, χ^2 for N measurements is equal to the sum of the square of the difference between the measured and theoretical values divided by the square of the uncertainties in measurements, σ. We express this relationship as

$$\chi^2 = \sum_{i=1}^{N} \frac{(O_m^i - O_t^i)^2}{\sigma_i^2}. \tag{40}$$

The brightness of astronomical objects is often reported in terms of the observed magnitude. For this reason, the χ^2 equation utilized in the following analysis compares the measured supernovae magnitudes to the theoretical magnitudes calculated from cosmological models. Magnitude measurements employ a logarithmic scale in which lower magnitude numbers indicate brighter objects. The theoretical magnitude of type Ia supernovae, m_t, is defined as a function of the luminosity distance, d_L:

$$m_t = 5 \log_{10}(d_L(z_s)) + \log_{10}(10\text{pc}). \tag{41}$$

The luminosity distance is derived from the energy relationship between absolute luminosity and flux. In general, if radiation is emitted with spherical symmetry, the conservation of energy dictates that the absolute luminosity of the source, L, be

related to the observed flux, F, by an inverse square law. If we treat the flux surface as a sphere of radius d then

$$\frac{f}{L} = \frac{1}{A(d)} = \frac{1}{4\pi d^2}, \tag{42}$$

where $A(d)$ denotes the area of the spherical flux surface. In the context of intergalactic distances, we set $d = r_s R_o$. The comoving distance from equation (3.15) is scaled by the absolute size of the Universe. However, the expansion of the Universe introduces two factors of $(1 + z_s)$ into the energy relationship of equation (5.3). One factor accounts for the energy loss of photons as the wavelength increases due to the expansion of space. Recall that the photon energy, E, depends on the wavelength, λ, according to the equation $E = hc/\lambda$. Additionally, individual photons emitted by the source arrive at the flux surface with a frequency reduced by a factor of $(1 + z_s)$. Thus,

$$L = 4\pi r_s^2 R_o^2 (1 + z_s)^2 F. \tag{43}$$

The luminosity distance is defined such that $L = 4\pi d_L^2 F$. Consequently, the luminosity distance can be expressed as a function of redshift. For traditional cosmological models, we have

$$d_L = (1 + z_s) r_s(z_s) R_o. \tag{44}$$

As previously mentioned, the χ^2 equation compares the observed supernovae magnitudes to the theoretical magnitudes calculated with various cosmological models. The observed supernovae magnitudes, μ_B, have been previously corrected to account for brighter-slower and brighter-bluer correlations in the Supernova Legacy Survey [2]. The quantities $\sigma(\mu_B)$ and σ_{int} denote the uncertainties associated with supernovae magnitude measurements and theoretical uncertainties in determining the intrinsic

luminosity of type Ia supernovae. Subsequent calculations set the theoretical dispersion uncertainty to $\sigma_{\text{int}} = 0.13$ in accordance with the Supernova Legacy Survey analysis [2]. After a series of substitutions, we develop a new χ^2 equation:

$$\chi^2 = \sum_{\text{objects}} \frac{(\mu_B - 5\log_{10}(d_L(z_s)) + \log_{10}(10\text{pc}) + \delta M)^2}{\sigma^2(\mu_B) + \sigma^2_{\text{int}}}. \tag{45}$$

The values of χ^2 prove to be extremely sensitive to the absolute magnitude used when calculating μ_B. Therefore, an additional paramter, δM, has been included in the χ^2 equation to assess the absolute magnitude scale difference between observation and theory. If the absolute magnitude scale used to calibrate values of μ_B corresponds closely to the reference magnitude used to calculate m_t, then we expect the fitted values of δM to be small for minimized χ^2.

For each particle physics theory, χ^2 is minimized numerically with respect to the relevant cosmological parameters. Next, confidence plots are created to illustrate the most probable regions of parameter space. Assuming that a given theory is correct, confidence plots show lines of equal probability that the actual parameter values of the Universe lie within a selected region of parameter space. The confidence intervals are generated by contours of one minus the p-value of the hypothesis:

$$1 - p = 1 - \int_{\Delta\chi^2(p_j)}^{\infty} f(x, n)dx. \tag{46}$$

The value of $\Delta\chi^2$ as a function of fitted parameters p_j is defined to be the difference between χ^2 evaluated at p_j and the minimized value of χ^2. We define

$$\Delta\chi^2(p_j) \equiv \chi^2(p_j) - \chi^2_{\text{min}}. \tag{47}$$

The probability density function, $f(x, n)$, for χ^2 tests with n degrees of freedom is given by

$$f(x,n) = \frac{x^{\frac{n}{2}-1}e^{-\frac{x}{2}}}{2^{\frac{n}{2}}\Gamma(\frac{n}{2})}. \tag{48}$$

The resulting tables of minimized χ^2 values and associated cosmological parameter values are contained in the results subsection for each theory. Relevant confidence plots are also included in each of the results subsections.

5.2 Results: Photon-Axion Oscillations

The inclusion of photon-axion oscillations modifies the luminosity-flux energy relationship given by equation (5.4) by removing a fraction of the photons arriving at the flux surface. The luminosity-flux relationship becomes

$$L = \frac{4\pi r_s^2 R_o^2 (1+z_s)^2 F}{P_{\gamma\to\gamma}(r_s(z_s)R_o)}. \tag{49}$$

Now the luminosity distance is reduced by the square root of the survival probability of photons. For photon-axion oscillations we have

$$d_L = \frac{(1+z_s)r_s(z_s)R_o}{P^{1/2}_{\gamma\to\gamma}(r_s(z_s)R_o)}. \tag{50}$$

In a first round of tests, χ^2 is minimized with respect to w_Λ, Ω_M, and δM for a Universe without photon axion oscillations. Our flat Universe assumption implies that $\Omega_M + \Omega_\Lambda = 1$. To include the possibility of photon-axion oscillations, χ^2 is minimized with respect to the additional decay length parameter, L_{dec}. The decay length parameter, L_{dec}, is a dimensionless scale factor such that the actual decay length of photons is equal to the product of L_{dec} and the theoretical decay length calculated by Csaki, Kaloper, and Terning. The results of these two tests are contained in Table 1.

In the next round of tests, we fix $w_\Lambda = -1$ based upon theory and repeat the procedure described above. The results of holding w_Λ constant are contained in Table 2. Notice that the best fit value for the decay length is large enough to render

	Control	Oscillations
χ^2	177.5	177.5
w_Λ	-0.670	-0.915
Ω_M	0.192	0.256
δM	-0.002	-0.002
L_{dec}		1.04 L_{th}

Table 1: The best fit for the photon-axion oscillations model is compared to a control case with no oscillations. The minimized χ^2 value and best fit cosmological parameters are shown above. The values were determined from 135 measurements of nearby and high-redshift type Ia supernovae ($N = 135$). L_{th} denotes the theoretical decay length of photons as predicted by Csaki, Kaloper, and Terning. Accordingly, we set $L_{th} = 3600$Mpc [6].

the effect of photon-axion oscillations negligible. Figures 2 and 3 contain confidence plots comparing the most probable values of cosmological parameters for models with and without photon-axion oscillations respectively.

A final confidence plot showing the supernovae constraints on the matter density and photon decay length is contained in Figure 4. In this plot, we have set $w_\Lambda = -1$. The region of high probability in parameter space shown in Figure 4 continues vertically off the figure as $\frac{L_{dec}}{L_th}$ becomes significantly greater than one. Recall from Table 2 that the best fit of parameters to supernovae data is located at $\Omega_M = 0.223$, $L_{dec} = 113$.

5.3 Results: Randall-Sundrum Braneworld Scenario

In the Randall-Sundrum braneworld scenario we can use the luminosity distance from equation (5.5) but now we add the possibility of shadow matter on the negative tension brane. The equation for a flat cosmology now becomes

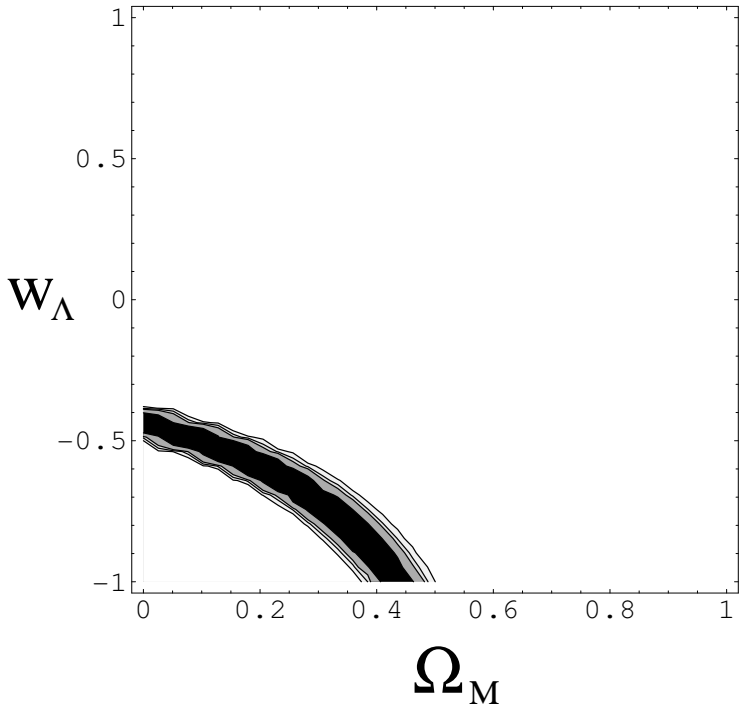

Figure 2: A confidence plot including photon-axion oscillations is shown above. The shaded regions indicate regions of parameter space where cosmological parameters as most likely to be located. The contour lines represent boundaries of the 0.68, 0.9, 0.95, and 0.99 confidence level regions. The number of degrees of freedom is equal to 133: 135 supernovae data points - 2 free parameters (Ω_M and w_Λ). We have set the photon decay length equal to the theoretical decay length suggested by Csaki, Kaloper, and Terning in the above plot above [6]. That is, $L_{dec} = L_{th} = 3600$Mpc.

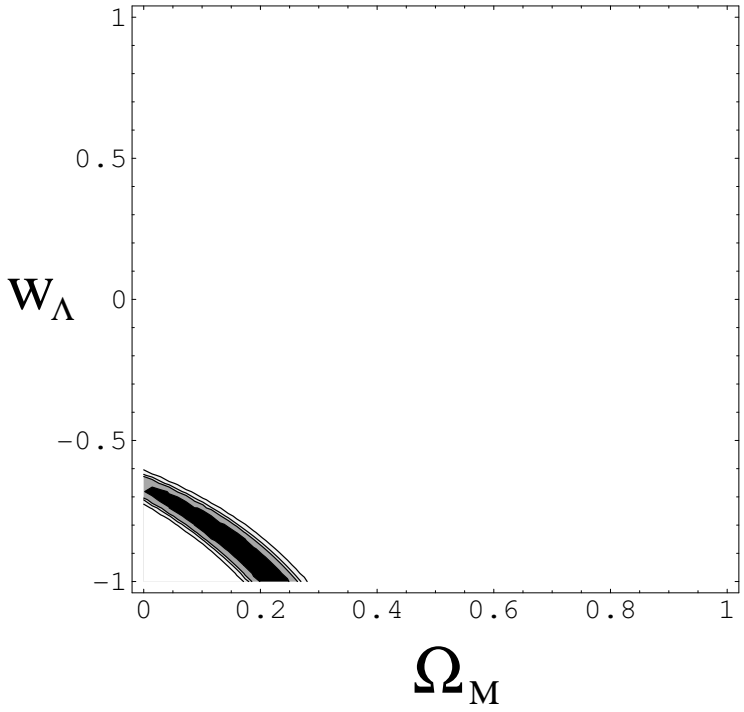

Figure 3: A confidence plot without photon-axion oscillations is shown above as a comparison to Figure 2. The shaded regions indicate regions of parameter space where cosmological parameters as most likely to be located. The contour lines represent boundaries of the 0.68, 0.9, 0.95, and 0.99 confidence level regions. The number of degrees of freedom is equal to 133: 135 supernovae data points - 2 free parameters (Ω_M and w_Λ).

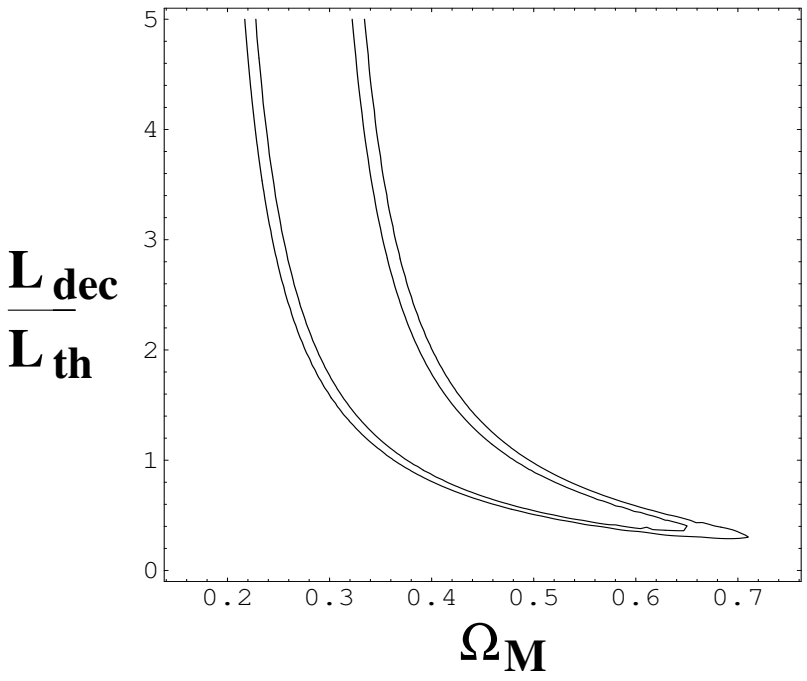

Figure 4: The confidence plot above shows the supernovae constraints to the matter density and decay length of photons in the photon-axion oscillation model. We have set $w_\Lambda = -1$. The contour lines represent boundaries of the 0.68, 0.9, 0.95, and 0.99 confidence level regions. The number of degrees of freedom is equal to 133: 135 supernovae data points - 2 free parameters (Ω_M and L_{dec}). L_{th} represents the theoretical photon decay length proposed by Csaki, Kaloper, and Terning. Accordingly, we set $L_{dec} = 3600$Mpc.

	Control	Oscillations
χ^2	177.6	177.6
Ω_M	0.228	0.230
δM	-0.006	-0.006
L_{dec}		113 L_{th}

Table 2: The best fit procedure is repeated setting $w_\Lambda = -1$. $\chi^2_{\rm min}$ and the associated cosmological parameters are shown above. The values were determined from 135 measurements of nearby and high-redshift type Ia supernovae ($N = 135$). L_{th} denotes the theoretical decay length of photons as predicted by Csaki, Kaloper, and Terning. As before, we set $L_{th} = 3600$Mpc [6].

$$\Omega_M + \Omega_{(-)} + \Omega_\Lambda = 1, \tag{51}$$

where Ω_M denotes the matter density on the positive tension brane, $\Omega_{(-)}$ represents the matter density on the negative tension brane, and Ω_Λ indicates the cosmological constant. In the statistical analysis, set $w_{(-)} = \frac{1}{5}$ and $w_\Lambda = -1$ and minimize χ^2 with respect to Ω_M, $\Omega_{(-)}$, and δM. The best fit of parameters in the Randall-Sundrum braneworld scenario is shown in Table 3.

5.4 Results: Topological Defects

The analysis of theories involving large scale topological defects will consist of two parts: first a discussion of cosmic strings followed by a study of domain walls. In both cases, the luminosity distance of equation (5.5) will be utilized and a flat cosmology is assumed. For the cosmic strings case, we have

$$\Omega_M + \Omega_{CS} + \Omega_\Lambda = 1, \tag{52}$$

where Ω_{CS} refers to the energy density of cosmic strings. The equation of state parameters are set $w_{CS} = -\frac{1}{3}$ and $w_\Lambda = -1$. Next, χ^2 is minimized with respect to

	Control	Shadow Matter
χ^2	177.6	177.5
Ω_M	0.228	0.375
δM	-0.006	-0.002
$\Omega_{(-)}$		-0.104

Table 3: The minimized χ^2 value and associated cosmological parameter fits for the Randall-Sundrum braneworld scenario are contained in the table above. The analysis sets $w_\Lambda = -1$ and $w_{(-)} = \frac{1}{5}$. The values were determined from 135 measurements of nearby and high-redshift type Ia supernovae ($N = 135$).

	Control	Cosmic Strings
χ^2	177.6	177.5
Ω_M	0.228	0.135
δM	-0.006	-0.002
Ω_{CS}		0.180

Table 4: The best fit of cosmological parameters for the cosmic strings case is shown above. In the analysis, $w_\Lambda = -1$ and $w_{CS} = -\frac{1}{3}$. The values were determined from 135 measurements of nearby and high-redshift type Ia supernovae ($N = 135$).

Ω_M, Ω_{CS}, and δM. Table 4 contains the results of this analysis. The confidence plot relating matter density and cosmic string energy density is shown in Figure 5.

The statistical analysis for the domain walls scenario procedes similarly. The flat cosmology assumption implies

$$\Omega_M + \Omega_{DW} + \Omega_\Lambda = 1, \tag{53}$$

where Ω_{DW} symbolizes the energy density associated with domain walls. Again, the cosmological constant equation of state parameter is set $\omega_\Lambda = -1$ and for domain

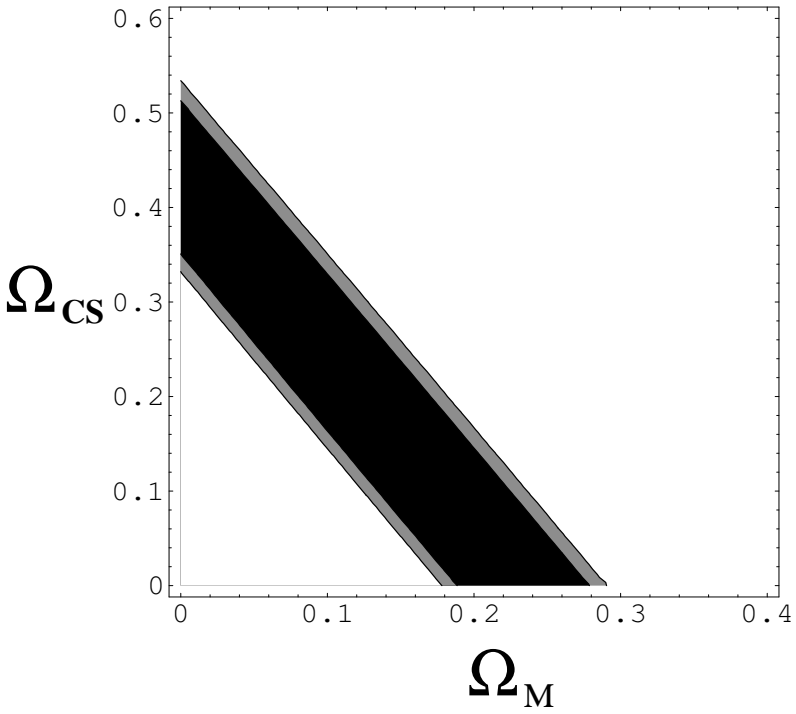

Figure 5: A confidence plot constraining parameters for a Universe containing cosmic strings in shown above. The shaded regions indication regions of paramter space where cosmological parameters are most likely to be located. The contours represent the boundaries of the 0.68, 0.9, 0.95, and 0.99 confidence level regions. The number of degrees of freedom is equal to 133: 135 supernovae data points - 2 free parameters. We set $w_\Lambda = -1$.

	Control	Domain Walls
χ^2	177.6	177.5
Ω_M	0.228	0.180
δM	-0.006	-0.002
Ω_{DW}		0.234

Table 5: The best fit of cosmological parameters for the domain walls case is shown above. In the analysis $w_\Lambda = -1$ and $w_{DW} = -\frac{2}{3}$. The values were determined from 135 measurements of nearby and high-redshift type Ia supernovae ($N = 135$).

walls, $w_{DW} = -\frac{2}{3}$. χ^2 is now minimized with respect to Ω_M, Ω_{CS}, and δM. See Table 5 for the results of this analysis. Figure 6 shows the supernovae constraints to matter density and domain wall energy density.

6 Conclusions

We constrained the free parameters of three theories motivated by particle physics. First, photon-axion oscillations are not preferred by recent type Ia supernovae data, but are allowed with sufficiently large photon decay length. Cosmology experiments such as the Sloan Digital Sky Survey and the Wilkinson Microwave Anisotropy Probe have already placed constraints on Ω_M that limit the role of photon-axion oscillations. The data of the Sloan Digital Sky Survey in conjuction with a theory of baryon acoustic oscillations finds that $\Omega_M = 0.256^{0.029}_{-0.024}$ (68 percent confidence level) [13]. By studying the cosmic microwave background radiation, WMAP limits the matter density of the Universe to $\Omega_M = 0.27 \pm 0.04$ [4]. In this slice of parameter space, the decay length of photons is bounded below by supernovae data so that $L_{dec} > 2L_{th} = 7200$Mpc. At this decay length, about twice the value proposed by Csaki, Kaloper, and Terning, the influence of photon-axion oscillations becomes less

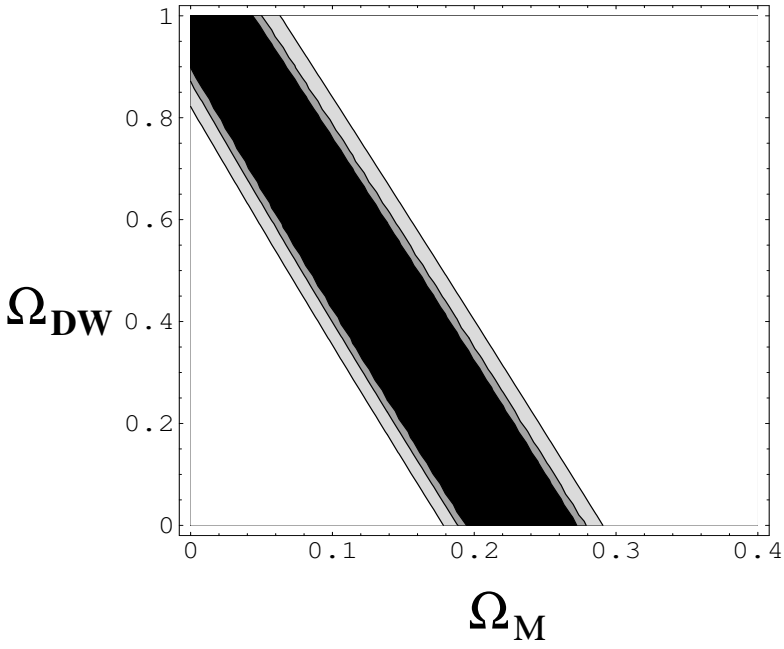

Figure 6: A confidence plot constraining parameters for a Universe containing domain walls in shown above. The shaded regions indication regions of paramter space where cosmological parameters are most likely to be located. The contours represent the boundaries of the 0.68, 0.9, 0.95, and 0.99 confidence level regions. The number of degrees of freedom is equal to 133: 135 supernovae data points - 2 free parameters. We set $w_\Lambda = -1$.

significant. However, photon-axion oscillations are still important to consider because if new cosmological experiments discover that $\Omega_M > 0.4$, then photon-axion oscillations are strongly perferred by type Ia supernovae data.

The supernovae data also confirms that substances with positive equation of state parameters are not allowed given our current understanding of cosmology. In the case of shadow matter on a negative tension brane with $w_{(-)} = \frac{1}{5}$, no density value of shadow matter improves the fit to supernovae data.

Finally, we examined the possibility that some component of the dark energy is composed of topological defects such as a network of cosmic strings or domain walls with equation of state parameters $w_{CS} = -\frac{1}{3}$ and $w_{DW} = -\frac{2}{3}$ respectively. We assumed that $w_\Lambda = -1$. When combining the analysis of type Ia supernovae data with studies of baryon acoustic oscillations and the cosmic microwave background, we find that $0.0 < \Omega_{CS} < 0.1$ and $0.0 < \Omega_{DW} < 0.2$ at the 68 percent confidence level. Thus, type Ia supernovae observations allow a density of domain walls comparable to the component of dark matter in the Universe.

References

[1] G.R. Farrar, R.A. Rosen, *A New Force in the Dark Sector?*, *Phys. Rev. Lett.* (2006), `astro-ph/0610298`.

[2] P. Astier, et al., *The Supernova Legacy Survey: Measurement of* Ω_M, Ω_Λ, *and* ω *from the First Year Data Set*, *Astronomy and Astrophysics* **447** (2006) 31, `astro-ph/0510447`.

[3] A.G. Riess, et al., *New Hubble Space Telescope Discoveries of Type Ia Supernovae at* $z > 1$*: Narrowing Constraints on the Early Behavior of Dark Energy*, *Astrophysics Journal* **656** (2006), `astro-ph/0611572`.

[4] D. Spergel, et al., *First Year Wilkinson Microwave Anisotropy Probe (WMAP) Observations: Determination of Cosmological Parameters*, *Astrophys. J. Suppl.* **148** (2003) 175, astro-ph/0302209.

[5] C. Csaki, N. Kaloper, J. Terning, *The accelerated acceleration of the universe*, *JCAP* **0606** (2006) 022, astro-ph/0507148.

[6] C. Csaki, N. Kaloper, J. Terning, *Dimming supernovae without cosmic acceleration*, *Phys. Rev. Lett.* **88** (2002) 161302, hep-ph/0111311.

[7] C. Csaki, N. Kaloper, J. Terning, *Effects of the intergalactic plasma on supernova dimming via photon axion oscillations*, *Phys. Lett.* **B535** (2002) 33, hep-ph/0112212.

[8] K. Jedamzik, V. Katalinic, A.V. Olinto, *A Limit on Primordial Small-Scale Magnetic Fields from CMB Distortions*, *Phys. Rev. Lett.* **85** (2000) 700, astro-ph/9911100.

[9] C. Csaki, J. Erlich, T.J. Hollowood, Y. Shirman, *Universal Aspects of Gravity Localized on Thick Branes*, *Nucl. Phys.* **B581** (2000) 309, hep-th/0001033.

[10] J. Garriga, T. Tanaka, *Gravity in the Randall-Sundrum Brane World*, *Phys. Rev. Lett.* **84** (2000) 2778, hep-th/9911055.

[11] A. Vilenkin, *Cosmic Strings and Other Topological Defects*, Cambridge University Press, Cambridge, 1994.

[12] A. Vilenkin, *Gravitational field of vacuum domain walls and strings*, *Phys. Rev.* **D23** (1981) 852.

[13] W. Percival, *Measuring the matter density using Baryon Accoustic Oscillations in the SSDS*, *ApJ* (2006), astro-ph/0608365v2.